Stratigraphic and Diagenetic Analysis of the Lower Cretaceous Lacustrine Microbialite Succession of the Yucca Formation along the Eastern Margin of the Chihuahua Trough, Indio Mountains, West Texas

Xiaowei Li and Katherine A. Giles

Institute of Tectonic Studies, Department of Geological Sciences, University of Texas at El Paso, El Paso, TX 79968

① Abstract

Successful hydrocarbon exploration in microbial carbonate reservoirs from Cretaceous rift basins along the South Atlantic margins has generated extensive interest in studies of lacustrine microbialite facies. In order to understand controls on reservoir and trap architecture in these complex systems, this study documents the petrographic attributes and stratigraphic architecture of lacustrine microbialite facies exposed in Lower Cretaceous strata in the Indio Mountains, West Texas. The Lower Cretaceous strata were deposited along the eastern margin of a NW-SE trending rift basin (Chihuahua Trough). The basin was inverted during the Laramide Orogeny exposing in cross section the former rift stratigraphy within three thrust panels. The Yucca Formation comprises the rift-fill sequence, which is transgressively overlain by shallow marine carbonate strata of the Bluff Mesa Formation. The lower member of the Yucca Fm. comprises mostly coarse-grained siliciclastic fluvial and alluvial facies. The upper member of the Yucca Fm. (focus of this study), contains interstratified fluvial siliciclastic and lacustrine facies.

Three distinctive types of microbialite facies are recognized in the upper member of the Yucca Fm.: (1) light gray to greenish microbial carbonate concretions set within reddish to light purple calcareous siltstone to mudstone matrix. Concretion interiors contain septarian-style fractures filled by coarse crystalline calcite and are often partially silicified. The concretion matrix shows multiple phases of replacement – detrital quartz replaced by euhedral dolomite and dolomite replaced by authigenic quartz; (2) stromatolitic bindstone with spherulites and nodular black chert; (3) light green thrombolite (~1cm across), locally dolomitized, within light purple siltstone to mudstone matrix. The three microbial facies are organized into 3 to 5m thick lacustrine cycles progressing upward from concretions, to stromatolites, to thrombolites. Each lacustrine cycle is bounded by fluvial siliciclastic facies. The lacustrine cycles are commonly erosionally terminated laterally by fluvial channels containing various clast types including microbialite facies. The cycles represent an upward increase in lake water depth and circulation, capped by baselevel fall and fluvial incision.

② Regional Geologic Setting

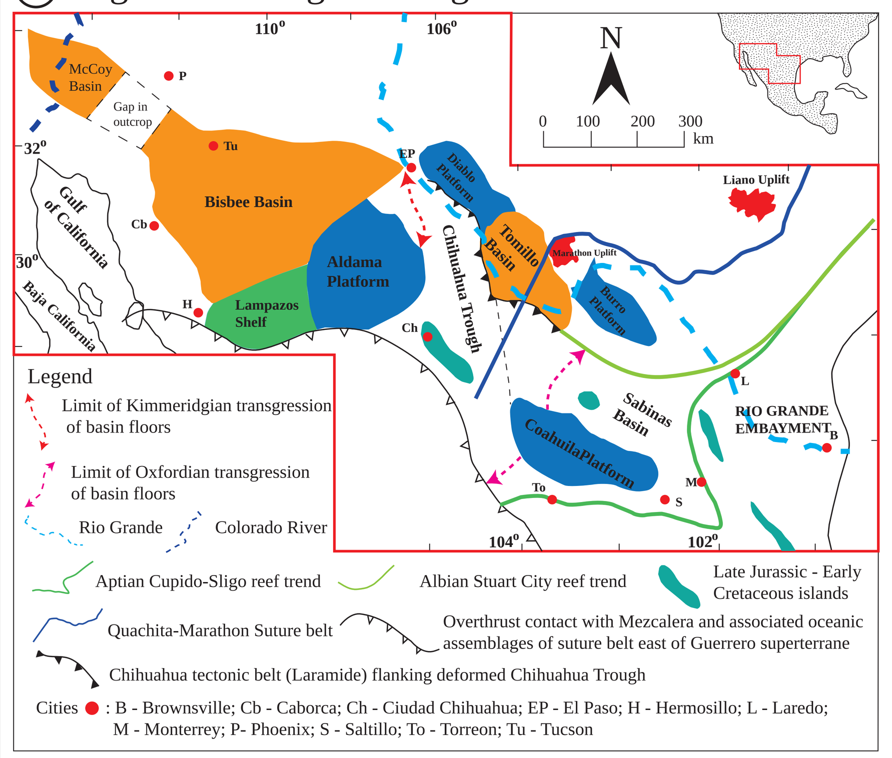

Fig. 1. Regional tectonic setting of Chihuahua Trough and associated basins of the US-Mexico border region. Revised after (Dickinson and Lawton, 2001) and its referred literatures.

③ Map of the Indio Mountains - Study Area

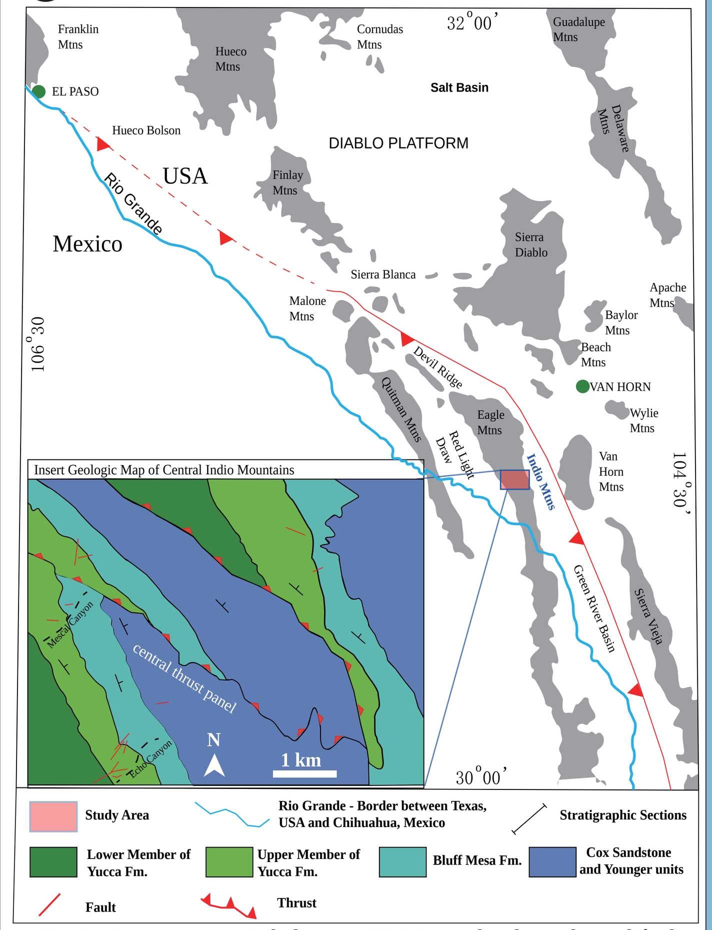

Fig. 2. Current mountain belts near US-Mexico border and simplified geologic map (insert figure) of the central Indio Mountains. Modified after Rohrbaugh (2001) and Page (2011).

④ Cretaceous Stratigraphy of the Indio Mountains

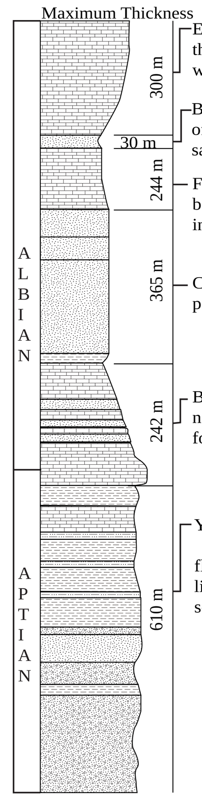

Espy Limestone: it mostly consists of medium to dark gray limestone, but the lower half contains shale with interbedded nodular limestone and marl with decreasing mollusk abundance upward.

Benevides Formation: it consists of two units. The lower unit is composed of shaley siltstone and the upper unit is identifiable by orange to brown sandstone with cross bedding and burrows.

Finlay Limestone: it is characterized by gray to dark gray, thick to massive beds (1 to 3m) with abundant bivalves and gastropods, and was deposited in a shallow shelf marine environment.

Cox Sandstone: it contains cross-bedded, fine- to medium-grained quartz arenite that was deposited in a coastal shallow-marine environment. On outcrop it displays pale-yellow to light-gray-weathering and is stained by iron-oxide.

Bluff Mesa Formation: it is characterized by gray to dark gray, fine-grained to crystalline, fossiliferous and oolitic limestone and quartz sandstone and is interpreted as normal marine deposition on a shallow shelf. Presence of the foraminifera *Orbitalina* is used to identify the Bluff Mesa Formation, because it is only present in this formation.

Yucca Formation

The Yucca Formation can be divided into distinct upper and lower members. The lower member comprises mostly coarse-grained, conglomerate-rich siliciclastic fluvial and alluvial facies. The upper member mainly comprises finer-grained fluvial conglomerate, sandstone, siltstone, and mudstone and lacustrine to marine limestone. The boundary between the upper Yucca and lower Yucca members in the field is identified by an abrupt fining-upward change from coarse-grained, poorly sorted conglomerate and conglomeratic sandstone to sandstone and siltstone interbedded with thin limestone.

Lithology: Conglomerate; Shale; Sandstone; Siltstone; Limestone

Figure 3. Simplified stratigraphic column and description of rock units in the Indio Mountains. Modified from Underwood (1962) and Rohrbaugh (2001).

⑤ Upper Member of Yucca Formation in the Central Thrust Panel of the Indio Mountains

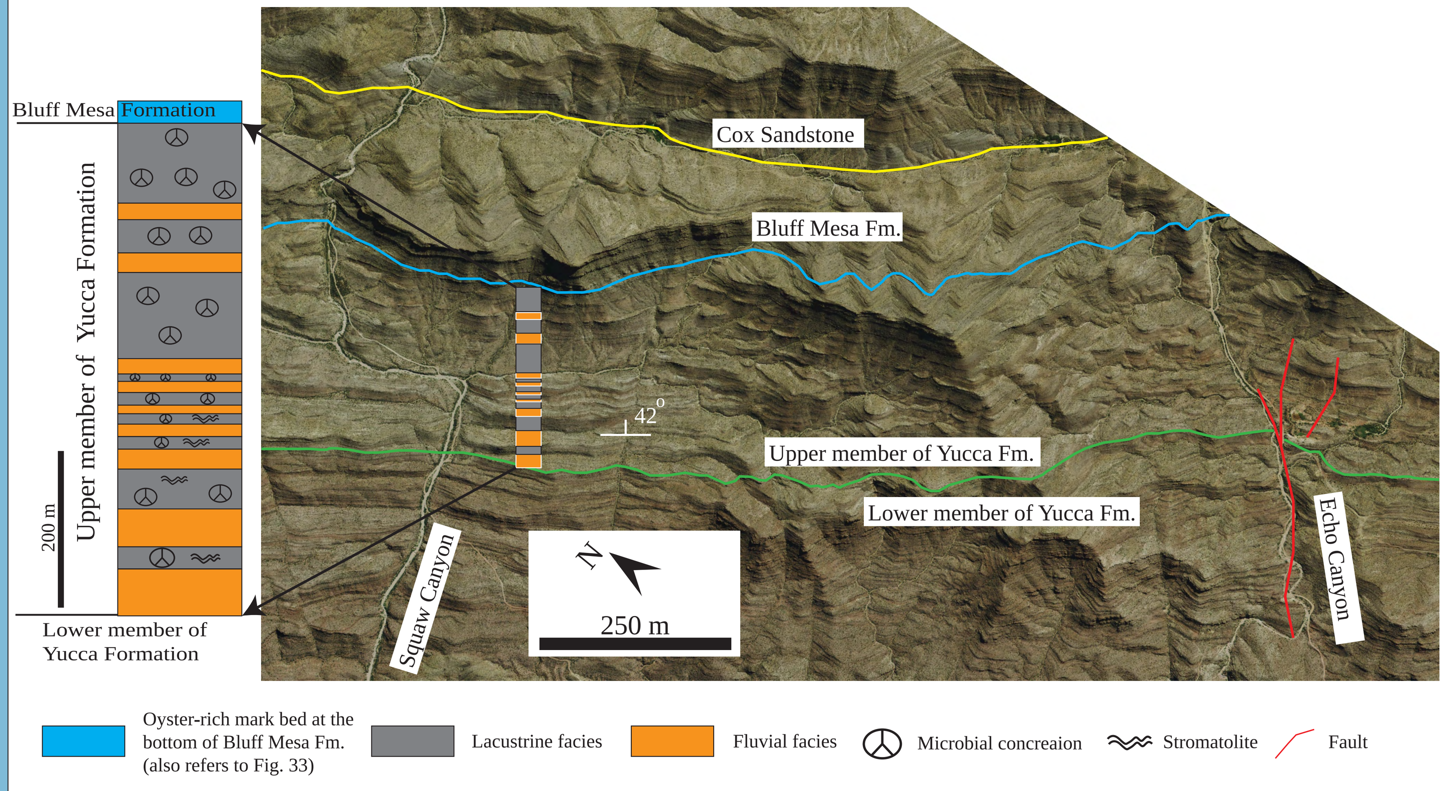

Fig. 4. Schematic stratigraphic column of lacustrine and fluvial facies cycles in the upper member of Lower Cretaceous Yucca Formation in the central thrust panel in the Indio Mountains (also refers to Fig. 2). Lacustrine facies appears to be slightly reddish and fluvial facies shows light gray on the satellite image between Echo and Squaw Canyons.

⑥ Upper Member of Yucca Formation Fluvial facies

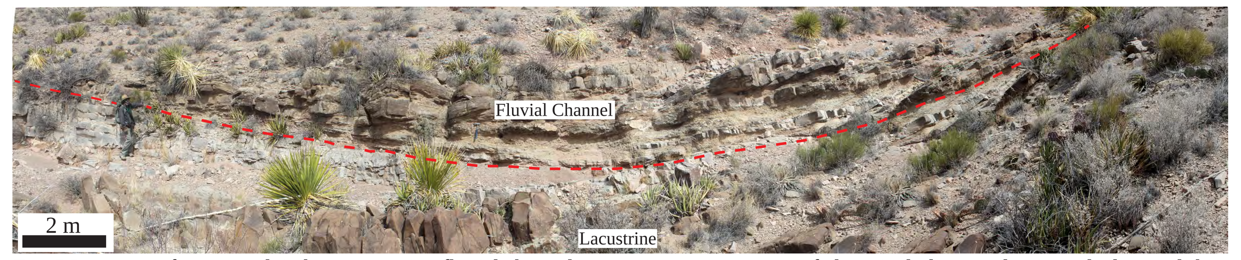

Fig. 5 Lacustrine facies overlain by a truncating fluvial channel containing various types of clasts including sandstone and siltstone lithic clasts, stromatolite (Figs. 6 and 7) and microbial concretions (Fig. 8).

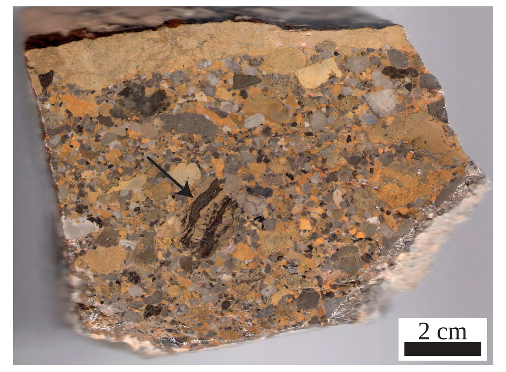

Fig. 6. Polished slab of channel deposits including various lithoclasts and a stromatolite clast (arrow).

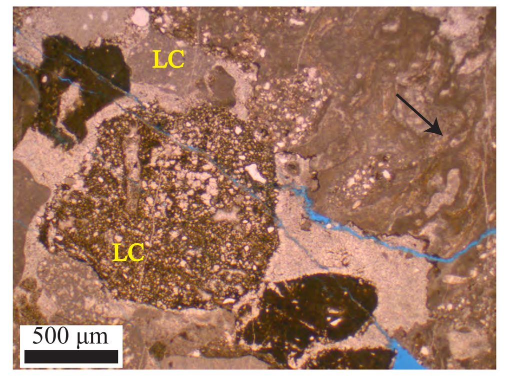

Fig. 7. Stromatolitic framework (arrow) and lithic clasts (LC) in channel deposits. Note dissolution creates secondary porosity.

Fig. 8. fluvial conglomerate containing various lithic clasts and microbial concretion with septarian-style fractures (arrows).

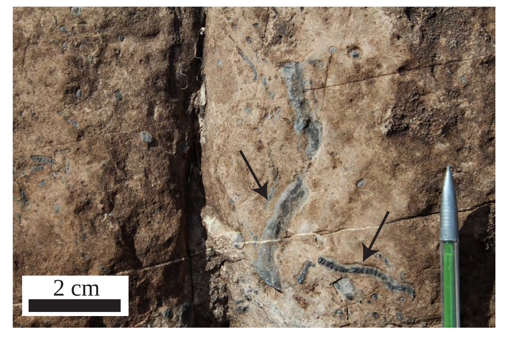

Fig. 9. Root traces (arrows) within fluvial sandstone.

Fig. 10. Ripple cross laminae in fluvial facies.

Fig. 11. Tabular cross-bedding in fluvial channel facies.

⑦ Upper Member of Yucca Formation Lacustrine Facies and Diagenetic Features

Microbial concretion

Fig. 12. Irregular gray microbial concretions within reddish siltstone and mudstone matrix (oblique view).

Fig. 16. Irregular yellowish microbial concretions with septarian-style cracks (arrow) within reddish siltstone and mudstone matrix (top view).

Diagenesis

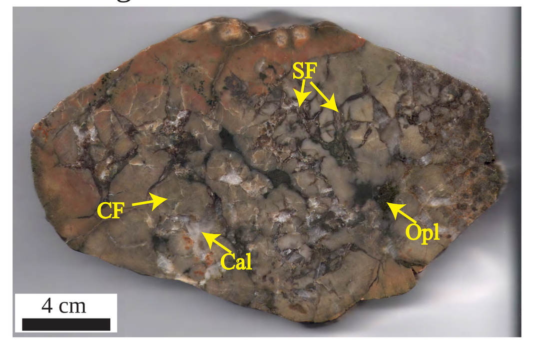

Fig. 13. A microbial concretion comprised of (1) internal septarian-style fracture (SF) filled by coarse crystalline calcite (Cal) and opal (Opl); (2) carbonate fans (see Fig. 15).

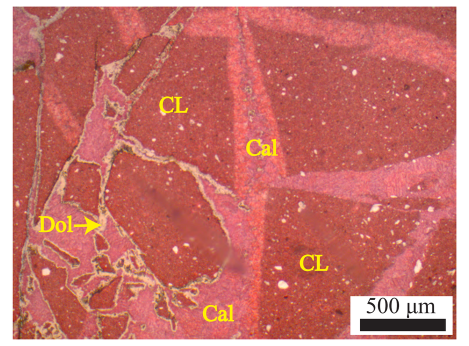

Fig. 14. Micrograph of Fig. 13. Micro-crystalline dolomite (Dol) rimming angular silt/mudstone clast (CL) separated by fractures filled by coarse crystalline calcite (Cal).

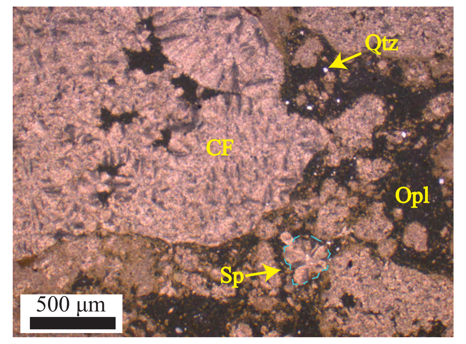

Fig. 15. Micrograph of Fig. 13. spherulite (Sp), calcite fans (CF) and detrital quartz (Qtz).

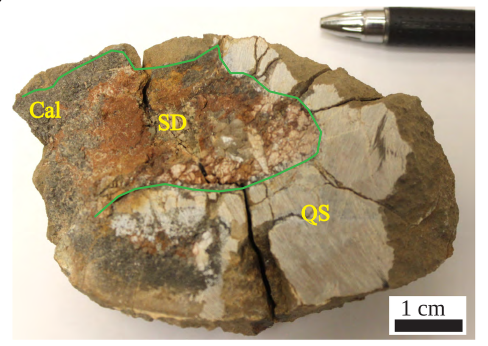

Fig. 17. A concretion primarily composed of quartz siltstone (QS). Calcite (Cal) and saddle dolomite (SD) cements subsequently fills in the central cavity of the concretion.

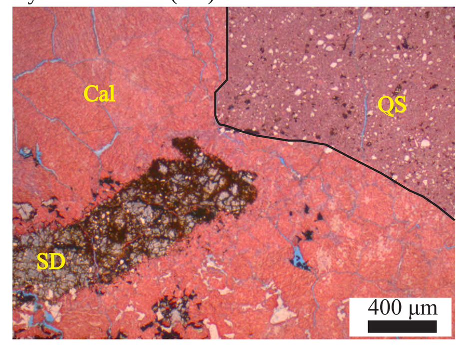

Fig. 18. Micrograph of Fig. 17. Occurrence of saddle dolomite suggests hydrothermal fluid influence. Secondary porosity is generated by dissolution.

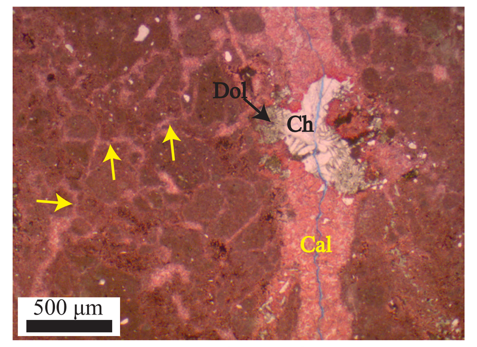

Fig. 19. Septarian-style fracture filled by calcite (Cal), silica (Ch) and dolomite cements (Dol). Concave-convex contact of lithic clasts reveals local brecciation (yellow arrows). Secondary porosity is also created by dissolution.

Reddish silt/mudstone matrix

Fig. 20. Irregular gray microbial concretions coalescencing together within reddish siltstone and mudstone matrix (side view).

Diagenesis

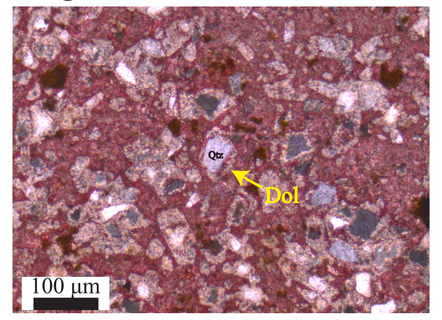

Fig. 21. Detrital quartz (Qtz) replaced by euhedral dolomite (Dol) in reddish silt/mudstone matrix.

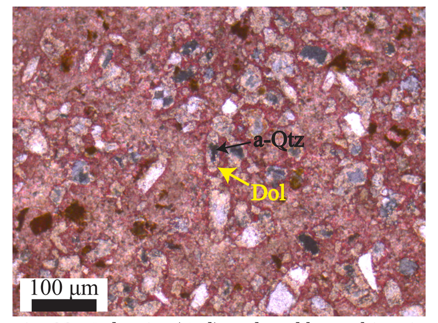

Fig. 22. Dolomite (Dol) replaced by authigenic quartz (a-Qtz) in reddish silt/mudstone matrix.

Stromatolite

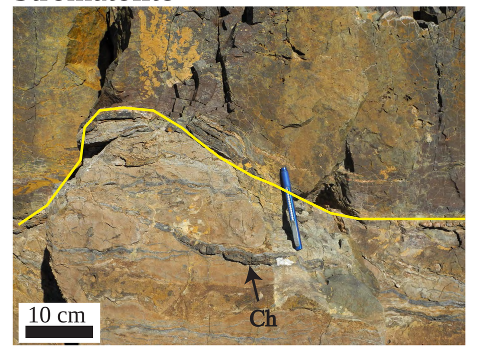

Fig. 23. Irregular black chert (Ch) and stromatolitic head (yellow curved line) overlain by light purple siltstone.

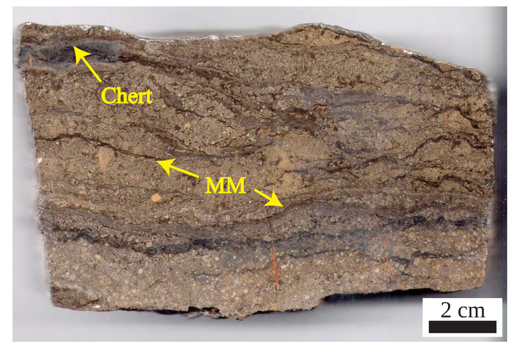

Fig. 27. Polished slab displaying dark partially silicified (chert) microbial mats (MM) that trap light yellowish siliciclastic sand/silt-sized materials.

Diagenesis

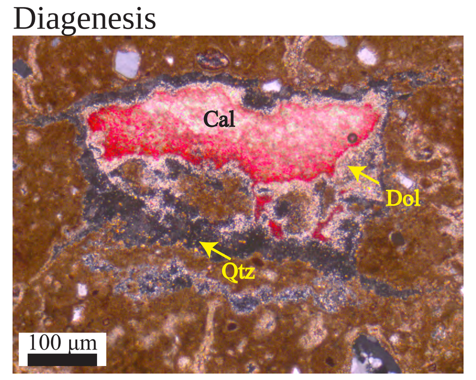

Fig. 24. Primary pores between microbial framework being subsequently filled by micro-quartz (Qtz), dolomite (Dol) and calcite (Cal).

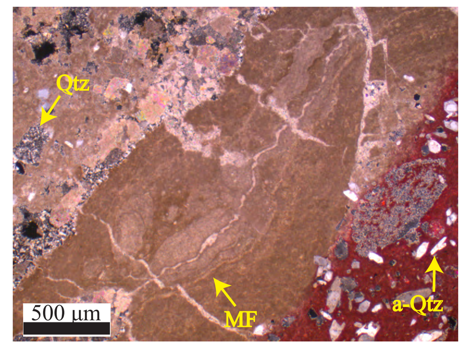

Fig. 25. Partially recrystallized microbial framework (MF). Note the authigenic quartz (a-Qtz) and calcite cement replaced by quartz (Qtz).

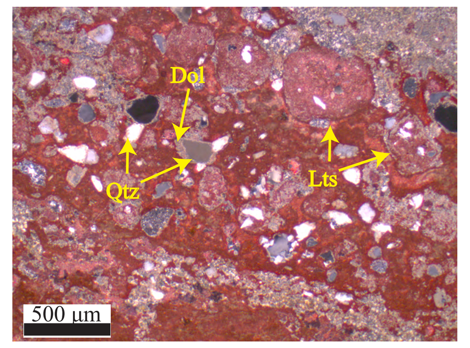

Fig. 26. subrounded to rounded lithoclasts (Lts) and detrital quartz (Qtz) between microbial mats. Note some quartz are rimmed by dolomite (Dol).

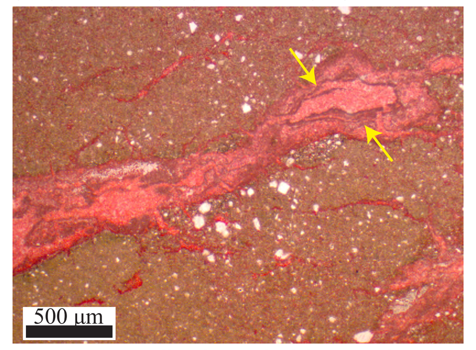

Fig. 28. Recrystallized microbial framework. Microbial framework is sometimes hard to identify because of strong recrystallization. Remnant filimentous structure of microbial mats is pointed by arrows.

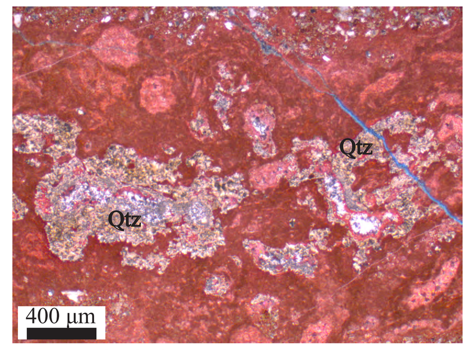

Fig. 29. Silicified microbial framework. Microbial framework is often silicified by micro-crystalline quartz (Qtz). Secondary porosity is created by dissolution.

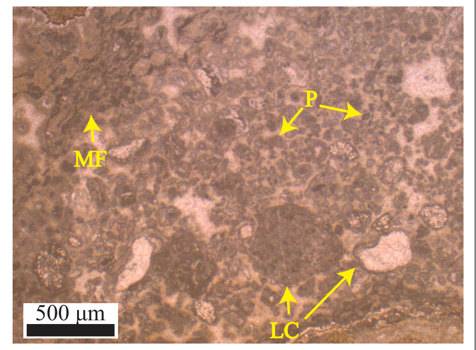

Fig. 30. Peloids (p) and recrystallized lithic clasts (LC) between microbial framework (MF).

Thrombolite

Figs. 31. Light green thrombolite (arrows) in light purple dolomitized siltstone present in another thrust panel of the Indio Mountains.

Diagenesis

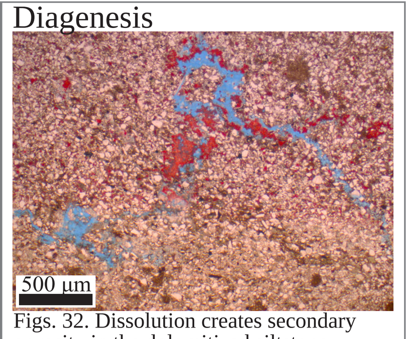

Figs. 32. Dissolution creates secondary porosity in the dolomitized siltstone.

⑧ Typical Facies of Bluff Mesa Formation - Normal Marine

Fig. 33. Fossiliferous lime pack/grainstone (mark bed in Fig. 4) containing marine fauna including oyster, gastropod, bryozoan and echinoderm.

Fig. 34. Oolitic grainstone with cross bedding and irregular chert bands (CB).

Table 1. Summary of diagenetic features of typical facies in the upper member of Yucca Formation

	Facies	GRAIN TYPES							POROSITY TYPES			CEMENT TYPES						DIAGENESIS					
		Lithoclast	In-situ brecciated clast	Chert	Quartz	Chalcedony	Clay	Fe-OXIDE	Stylolite-dissolution	Fracture	inter-gradular	Calcite	Dolomite	Quartz	chalcedony	Chert	Opal	Dolomitization	SILIFICATION Chert	SILIFICATION Quartz	Stylolite	Spherulite	Radial carbonate fan
Lacustrine	Microbial concretion		X	X	X			X	X	X		X	X			X	X	X			X	X	X
Lacustrine	Reddish silt/mudstone matrix	X		X	X			X	X			X	X					X		X	X		
Lacustrine	Stromatolite			X	X	X			X	X		X	X	X				X		X	X		
Lacustrine	Thrombolite	X, very few		X	X		X, very few	X	X			X	X	X		X		X			X		
Fluvial	Siliciclastic facies	X		X	X	X	X	X	X	X	X	X	X very local		X	X		X	X		X		

⑨ Conclusion

- The upper member of the Yucca Formation primarily consists of fluvial and lacustrine facies that can be traced laterally and distinguished on satellite image.
- Each lacustrine cycle, 3-5 m thick, progresses upward from (1) microbial concretions in reddish silt/mudstone matrix; to (2) stromatolite with irregular chert nodules; to (3) thrombolite in light purple silt/mudstone matrix which is not present in the central thrust panel of the Indio Mountains.
- Lacustrine cycles show a shallowing-upward trend due to base-level dropping and is capped by fluvial facies.
- Microbial concretions become dominant in lacustrine cycles stratigraphically upward.
- Microbial concretions are primarily composed of silt/mudstone lithic clasts with small amount of detrital quartz. Their internal septarian-style fractures are filled by (1) coarse crystalline calcite that is usually replaced by silica cements (opal, chert and quartz); (2) mainly micro-crystalline quartz/chert, dolomite, carbonate fans (calcite) and occassionally by spherulites; (3) coarse-crystalline calcite and saddle dolomite.
- Reddish silt/mudstone matrix reveals multiple phases of replacement - detrital quartz replaced by euhedral dolomite and dolomite replaced by authigenic quartz.
- Depositional primary porosity in microbial concretions, stromatolite and thrombolite is low, <5% in average, which is caused by occlusion by cements of micro-crystalline quartz, opal, dolomite and calcite. The secondary porosity network in lacustrine facies is mainly enhanced by dissolution and fracture during late burial stage.
- Diagenetic features in fluvial facies are similar to the reddish silt/mudstone matrix.

⑩ Further Work

- Geochemical analysis of microbial concretion to enhance interpretaion of its genesis.
- Detailed mapping of facies between Squaw and Echo Canyons in order to:

  (1) Verify the depositional scale and distribution of microbialite sub-facies and whether microbial sub-facies vary laterally between Squaw and Echo Canyons.

  (2) Analyze the depositional controls including syndepostional faulting on stratigraphic framework between Squaw and Echo Canyons.

  (3) Understand whether different diagenetic alterations preferentially occur in different facies; if and how the diverse types of diagenetic features change laterally and vertically and their impacts on depositional primary porosity as to the proximity to faults (syndepositional?) between Squaw and Echo Canyons.

⑪ Selected References

1. Dickinson, W.R. and Lawton, T.F., 2001, Tectonic setting and sandstone petrofacies of the Bisbee basin (USA-Mexico): Journal of South American Earth Sciences, v. 14, p. 475-504.
2. Haenggi, W.T., 2002, Tectonic history of the Chihuahua trough, Mexico and adjacent USA, Part II: Mesozoic and Cenozoic: Boletin De La Sociedad Geologica Mexicana, Tomo LV, Num. 1, p. 38-94.
3. Natalicchio, M., Birgel, D., Dela Pierre, F., Martire, L., Clari, P., Spötl, C., Peckmann, J., 2012, Polyphasic carbonate precipitation in the shallow subsurface: insights from microbially-formed authigenic carbonate beds in upper Miocene sediments of the Tertiary Piedmont Basin (NW Italy): Palaeogeography, Palaeoclimatology, Palaeoecology, v. 329-330, p. 158-172.
4. Page, S.J., 2011, Fold-thrust system overprinting syn-rift structures on the margin of an inverted rift basin: Indio Mountains, West Texas: Thesis, The University of Texas at El Paso, p. 3-17.
5. Underwood, J.R., 1962, Geology of the Eagle Mountains and Vicinity, Hudspeth County, Texas: Dissertation, The University of Texas at Austin, p. 167-169.

Acknowledgement

This work is funded by ITS salt-tectonics consortium member:

AAPG Harold J. Funkhouser Grant (Grant-in-Aid).

Special thanks are also extended to Nila Matsler, Jonathan E. Stautberg, Pawan Budhathoki and Richard Langford.